field energy. The gravitational mass (and energy) resides entirely at the position of the singularity. However, when P_4 is computed for the purely gravitational field by the use of "isotropic" coordinates,[6] one obtains

$$P_4=mc^2(1-\kappa m/2rc^2). \quad (36)$$

[6] R. C. Tolman, *Relativity, Thermodynamics and Cosmology* (Clarendon Press, Oxford, England, 1934), Eq. (82.14), p. 205.

By a mere change of the coordinate system we have achieved a field in which part of the gravitational mass resides in the field. Only if viewed from an infinite distance does P_4 yield the total mass, m, of the singularity.

The author wishes to express his sincere gratitude to Professor Peter Bergmann, who suggested this problem

PHYSICAL REVIEW VOLUME 81, NUMBER 6 MARCH 15, 1951

Electron Loss Cross Sections for Hydrogen Atoms Passing through Hydrogen Gas

J. H. MONTAGUE
Department of Physics and Institute for Nuclear Studies, University of Chicago, Chicago, Illinois
(Received November 7, 1950)

Measurements have been made of the electron loss cross section in hydrogen gas for hydrogen atoms moving with kinetic energies between 45 kev and 329 kev. At these two limiting energies the values of the cross section were $6.6_6\times10^{-17}$ cm^2 and $2.2_1\times10^{-17}$ cm^2, respectively, with an error of plus or minus 10 percent. Between 120 kev and 329 kev the cross section was found to vary approximately as E^n, where E is the kinetic energy of the atom, and n is -0.70 ± 0.05.

I. INTRODUCTION

STUDIES of electron capture and loss by light ions passing through matter are of interest for a more complete understanding of the phenomena themselves, and are necessary for an interpretation of experimental range-energy curves at low energies. Furthermore, they are of interest in that they play an important role in the stopping of fission fragments, where the charge of the fragment plays an important part.

General surveys of the work done on capture and loss have been given by Knipp and Teller[1] and by Bohr.[2] Previous experimental investigations have been made using either hydrogen canal rays,[3–6] or high energy alpha-particles from radioactive sources.[7–9] Consequently, for particle energies of from 25 kev to about one Mev few data are available. Recently, Hall[10] has helped to fill this gap by his study of the ratio of the charged to neutral component in hydrogen ion beams of energies between twenty and four hundred kev passing through metallic media. The present paper gives values of the electron loss cross section in hydrogen for hydrogen atomic beams with energies in about the same range.

In this experiment a collimated beam of protons was passed through a thin aluminized-nitrocellulose window into an electron-exchange chamber, which could be evacuated to a pressure at which the mean free path for collision was more than ten times the diameter. The beam emerging from the window consisted of both a charged and a neutral component, owing to capture and loss processes taking place in the window material. The charged particles were deflected away by a magnetic field in which the electron-exchange chamber was situated; the neutral particles, however, continued across the chamber and into a detector.

When hydrogen gas at low pressure was introduced into the chamber, some of the moving atoms in the neutral beam lost their planetary electron in collisions with the hydrogen atoms in the gas, and were then deflected by the magnetic field so that they no longer entered the detector. Assuming that all neutral particles which undergo a charge change will fail to enter the detector (this assumption will be examined more critically later), it is clear that the number of particles $N(p)$ arriving at the detector when the electron-exchange chamber is filled with hydrogen gas at a pressure p millimeters of mercury is given by

$$(p)\equiv N(p)/N(0)=\exp(-N(p)\sigma_l d) =\exp[(-19.21\times10^{18}p\sigma_l d)/T], \quad (1)$$

where $N(0)$ is the number of particles entering the detector when the chamber is evacuated, $n(p)$ is the number of atoms per cc in the gas, T is the absolute temperature of the gas, d is the path length for the moving particles (i.e., the distance from the entrance window to the detector), and σ_l is the electron loss cross section per atom of hydrogen for atoms of the energy under consideration.

[1] J. Knipp and E. Teller, Phys. Rev. **59**, 659 (1941).
[2] N. Bohr, *The Penetration of Atomic Particles through Matter* (Det. Kgl. Danske Videnskabernes Selskab, 1948).
[3] E. Ruchardt, Ann. Physik **71**, 377 (1923).
[4] A. Ruttenauer, Z. Physik **4**, 267 (1921).
[5] H. Bartels, Ann. Physik **13**, 373 (1932).
[6] H. Meyer, Ann. Physik **30**, 635 (1937).
[7] E. Rutherford, Phil. Mag. **47**, 277 (1924).
[8] P. Kapitza, Proc. Roy. Soc. (London) **106**, 602 (1924).
[9] G. Henderson, Proc. Roy. Soc. (London) **109**, 157 (1925).
[10] T. Hall, Phys. Rev. **79**, 504 (1950).

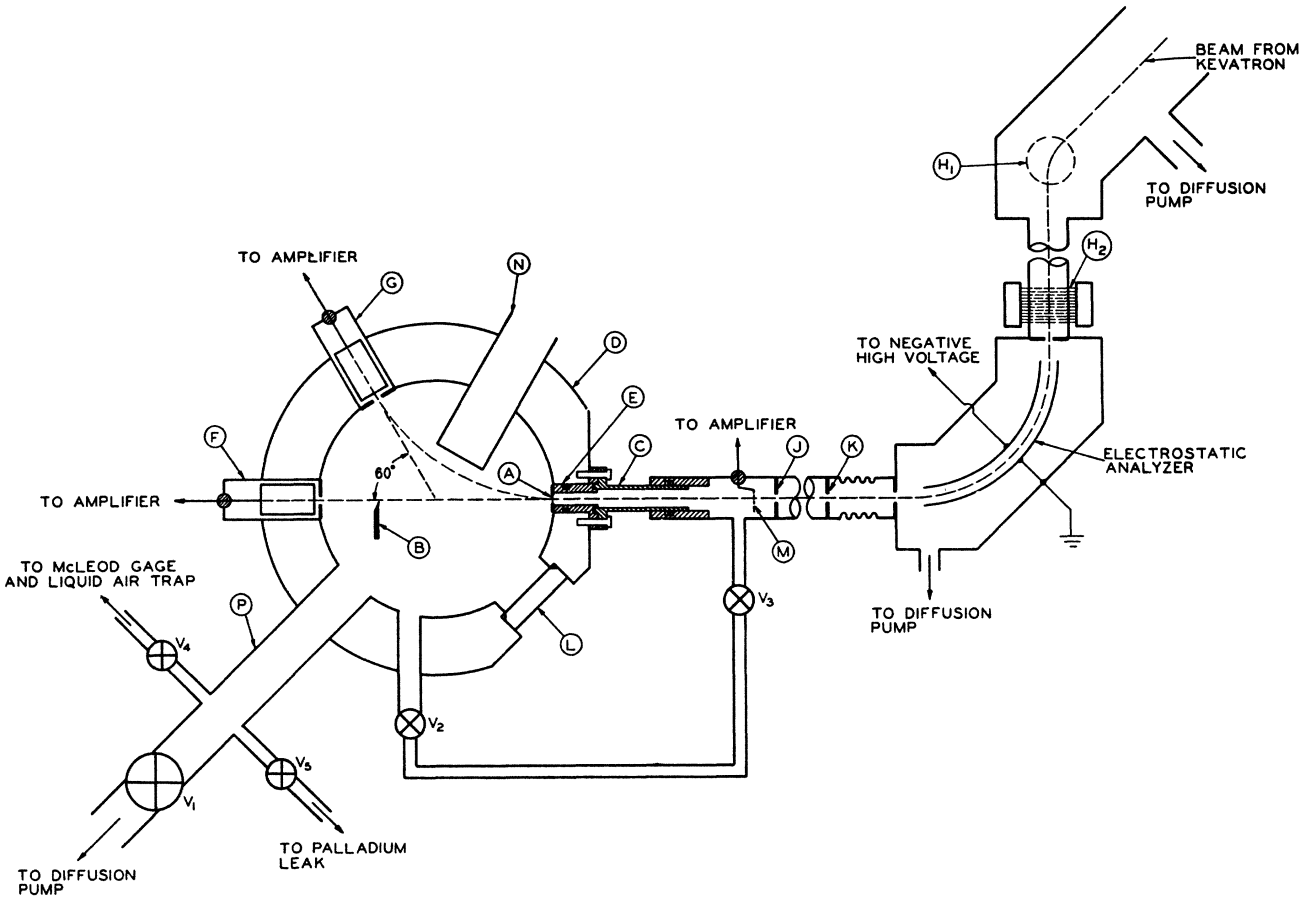

FIG. 1. Apparatus, schematic.

II. DESCRIPTION OF THE APPARATUS

Figure 1 is a schematic diagram of the experimental arrangement; the items labeled by letters in the figure will be identified and referred to in the following paragraphs.

(A) Production and Collimation of the Proton Beam

The source of energetic hydrogen ions was the University of Chicago 400-kev Cockcroft-Walton accelerator, or kevatron, which is described elsewhere.[11–13] The kevatron beam was first analyzed by the vertical magnetic field H_1 (Fig. 1) and the selected component (either the proton beam or the molecular-hydrogen-ion beam) directed down a 1.28-meter tube to the entrance of an electrostatic analyzer. Accurate positioning of the beam was accomplished by adjustments of the magnetic field H_1 and of the weak horizontal magnetic field H_2. The purpose of the electrostatic analyzer was to provide an accurate estimate of the beam energy in terms of the potential difference between the deflecting plates necessary to bend the beam around the analyzer and into the collimating assembly. This analyzer was one which has been described previously in the literature;[12,14] for this experiment it was calibrated against another electrostatic analyzer used in this laboratory, the construction and calibration of which have been given elsewhere.[15]

After leaving the electrostatic analyzer, the ion beam passed into the collimating assembly. This consisted of two circular brass diaphragms, J and K, with openings 0.158 cm in diameter, separated by 13.33 cm. The collimating tube was connected to the output of the analyzer by a flexible coupling for ease in alignment. From the collimator the beam travelled a distance of about 10 cm to the entrance window A, and through it into the electron-exchange chamber. An insulated monel wire screen M of 34 percent transmission was located just beyond the final collimating diaphragm and was used to collect a portion of the beam for monitoring purposes. The amount of beam so collected was usually between 0.05×10^{-2} and 1×10^{-2} μamp. An

[11] Allison, del Rosario, Hinton, and Wilcox, Phys. Rev. **71**, 139 (1947).
[12] L. del Rosario, Phys. Rev. **74**, 305 (1948).
[13] A. H. Morrish, Phys. Rev. **76**, 1653 (1949).
[14] Allison, Skaggs, and Smith, Phys. Rev. **57**, 550 (1940).
[15] Allison, Frankel, Hall, Montague, Morrish, and Warshaw, Rev. Sci. Instr. **20**, 735 (1949).

electrical connection was brought from the screen through the vacuum wall by a Kovar-glass seal and thence to the input of a direct-current amplifier of standard type;[16] the output of the amplifier was fed to a mirror galvanometer. The sensitivity of the whole arrangement was easily adjustable to cover a wide range of amplifier input currents by changing a resistance in series with the galvanometer. Tests showed that the galvanometer deflection varied linearly with the amplifier input current over its entire usable range for galvanometer series-resistances from zero to two megohms. This corresponds to a maximum input grid-voltage of three volts above ground.

During the experiment it was only required that, for a given beam energy, the monitor galvanometer deflection should be proportional to the strength of the collimated beam. Thus, it was not necessary to take into account the emission of secondary electrons from the monitor screen, although this effect undoubtedly existed.

(B) The Entrance Window

The aluminized-nitrocellulose entrance window, which provided the neutral beam for the experiment and also served as a vacuum seal between the electron-exchange chamber vacuum and that of the electrostatic analyzer, consisted of a film of nitrocellulose,[17] about 0.01 mg/cm^2 thick, over which a layer of aluminum (also about 0.01 mg/cm^2) had been evaporated. It was mounted on the end of a window holder, E, which fitted into the side of the electron-exchange chamber wall. A flange on the end of the window holder opposite that on which the window was mounted bolted to a sliding coupling C, which facilitated the changing of windows. Since the windows were very fragile, a bypass line (between valves V_2 and V_3 in Fig. 1) was provided in order to eliminate pressure differences across the window during evacuations.

The aluminum coating on the window was in electrical contact with the window holder and prevented the building up of charge on the window as the beam passed through it. At first, windows without such conducting aluminum layers were used and it was found that they quickly broke when bombarded by a beam, even when their thickness was as high as 0.03 mg/cm^2. The aluminum prevented such breakages, however, and some of the foils coated with it have lasted as long as seventy-five hours under the proton beam.

(C) The Electron-Exchange Chamber

The electron-exchange chamber was a hollow cylinder of bronze, 3.17 cm high, the top and bottom of which were closed by brass plates. The inner diameter of the cylinder was 12.70 cm, which was exactly the same as the diameter of the two magnet pole-faces between which the chamber rested. The bottom cover plate was shaped to fit snugly over the lower pole face; this device positioned the chamber so that its vertical axis coincided with that common to the two magnet poles.

In the circular wall of the chamber, and diametrically opposite to one another, were situated the window holder E and the detector F. Detector G was identical with detector F and was located so that its axis made an angle of sixty degrees with the mutual axis of E and F, and shown in Fig. 1. Both detectors and the window holder were easily removable, as the vacuum seals to the electron-exchange chamber were made with O-rings.

The plane containing the axes of E, F, and G lay halfway between the magnet pole faces. The entrance window A and the entrance apertures of the detectors were located between the edges of the poles. Thus, the paths of particles which travelled from A to the entrance of either detector lay entirely between the pole faces and so were subject to a fairly constant magnetic field throughout their length. The path of a charged particle traveling from A to detector G under the action of the magnetic field is shown in Fig. 1 as a broken circular arc; it has a radius of curvature of 11.0 cm.

The chamber wall also contained an observation window L, an internal can N which permitted the introduction of a fluxmeter into the region between the magnet pole faces, and the bypass valve V_2. A brass baffle B was located inside the chamber, as shown in Fig. 1, at a distance of 0.1 cm from the common axis of F and E, and 3.25 cm from the entrance to F. Its purpose, which will be explained more fully later, was to lessen the effect of scattering in the entrance window upon the experimental measurements.

Evacuation of the chamber, and the introduction of hydrogen gas into it, was accomplished through the manifold P, which is shown very schematically in Fig. 1. The manifold was connected by a large sylphon vacuum valve V_1 to a liquid-nitrogen trap and an oil diffusion pump which evacuated the electron-exchange chamber to better than 10^{-4} mm Hg. Valve V_4 leads to a second liquid-nitrogen trap and a McLeod gauge, which was used to measure the gas pressure in the electron-exchange chamber. Hydrogen gas was let in through valve V_5 from a palladium leak. This method both purified the gas and allowed it to be let in slowly. In practice the leak was allowed to run continuously, and when sufficient hydrogen gas was in the deflection chamber, the valve V_5 was closed.

When valves V_1 and V_5 were closed, the McLeod gauge indicated a pressure rise of 4×10^{-4} mm Hg/hour in the electron-exchange chamber; this rise rate was practically independent of whether or not the cold trap was used. During the experiment the chamber was

[16] The circuit is given on the data sheet for the Raytheon CK5697/CK570 electrometer triode, published by the Raytheon Manufacturing Company, Newton, Massachusetts.

[17] The nitrocellulose films were prepared from Zapon Aquanite-A Lacquer by a standard technique.

never left closed off for more than fifteen minutes before re-evacuation. Since hydrogen pressures above 1×10^{-2} mm Hg were used in the chamber, the effect on the measured cross sections of such a leakage rate was negligible.

(D) The Detectors

The detectors were of a type which measured the strength of a proton or atomic beam in terms of the secondary electron current produced when the beam struck a beryllium-copper collector plate.[18] A cutaway view of one of the detectors is shown in Fig. 2. For the detection of particles the collector plate U was connected with one used for monitor current and was biased 67.5 v negatively with respect to ground. Since the long axis of U was oriented at 10.0° to the horizontal, the direction of the resulting electric field between U and the grounded electrode W (whose lower face was parallel to plate U, and separated from it by 0.32 cm) was nearly parallel to that of the magnetic field around the detector. Thus, all secondary electrons emitted when a moving proton or neutral atom impinged on the beryllium-copper were pulled to W and so gave an effective positive current to the collector plate. The magnetic field restricted any horizontal motion of the electrons to tight spirals and thus served to trap them between U and W. It should be noted that the internal geometry of the detector was such that any beam particle passing through the detector's entrance aperture and moving in a horizontal path would strike the plate U. The entrance aperture used in the present measurements was 0.32 cm high by 0.147 cm wide. The detector itself was of 2.22 cm diameter and 9.8 cm over-all length.

It was found that, for a given beam current entering the detector, the detector response was independent of the negative bias voltage applied to the collector plate for voltages in the range from forty-five volts to above three hundred volts. Thus, with the −67.5-v bias used in this experiment the detector was operating well within its saturation region. As regards other properties of the detector it should be noted that each loss cross section was completely measured at a constant value of the magnetic field. Thus, it was only necessary to show that the detector response is directly proportional to the number of ions or atoms striking the surface per second, and that a correction can be experimentally made for any effect of the hydrogen gas, when admitted, on the detector sensitivity. The investigation of these points is described in a later section of this paper.

(E) The Magnetic Field

The magnetic field was generated by an electromagnet, the current supply for which was a 110-v dc generator-ac motor set used only for this purpose.

[18] Beryllium-copper was chosen because of its high electron multiplication. J. S. Allen, Rev. Sci. Instr. **18**, 739 (1947).

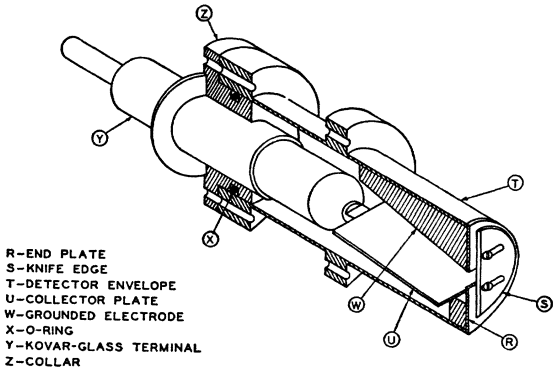

FIG. 2. Cutaway view of detector.

Fields as high as 10^4 gauss could be obtained, and were measured approximately with a generating fluxmeter which fitted into the can N. The fluxmeter was driven by a synchronous motor and gave readings reproducible to about 3 percent. It was used as a rough monitor for the field, and also for indicating when the magnetic field was zero.

It was found necessary to shield the collimator and adjacent parts from the magnet's leakage flux, which was quite intense. Since the window holder was enclosed by the electron-exchange chamber wall, it could not be externally shielded. It was made of Armco iron, however, in order to provide as much shielding as possible. The sliding coupling C was also made of Armco, so as to give some extra shielding.

III. EXPERIMENTAL METHODS

(A) Measurement of Proton Energy after the Entrance Window

Measurements were first made of the deflecting magnet currents necessary to bend protons of various energies into the sixty-degree detector G. For this work the entrance window W was removed and the electron-exchange chamber was evacuated to less than 2×10^{-4} mm Hg pressure. The proton energies were determined with the electrostatic analyzer, and the magnet current corresponding to the peak detector-current was read several times. Independent trials were found to agree within better than 2 percent. Hysteresis effects were taken into account by zeroing the magnetic field before each trial with the aid of the generating fluxmeter, and by never decreasing the magnet current during a measurement (these precautions were observed throughout the experiment).

The apparatus could now be used as a magnetic energy-analyzer for determining the energy of the protons after they had passed through the entrance window; such a measurement was made before each cross-section determination. A profile of normalized detector current r_G *versus* magnet current was taken with the electron-exchange chamber evacuated to less than 2×10^{-4} mm Hg. The quantity r_G is here defined

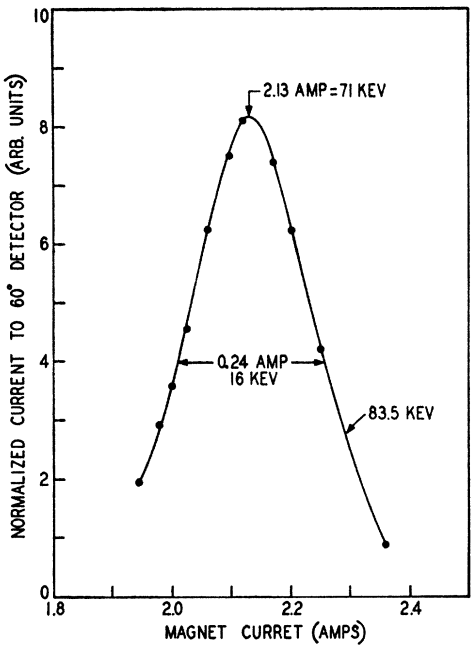

FIG. 3. Plot of 60° detector current *versus* magnet current for a 167-kev molecular hydrogen-ion beam incident on the window. The peak gives a mean energy of 71 kev after the window.

as the ratio of the sixty-degree detector current to the monitor current. From the magnet current at the peak of the profile the energy of the protons on leaving the window was determined.

A typical profile is shown in Fig. 3; the particles incident on the window were molecular-hydrogen ions of 167-kev energy, each of which was equivalent, for purposes of this experiment, to two protons of 83.5-kev energy. The peak of the profile was at 2.13 amp, which gives a proton energy of 71 kev after the window. The width of the profile at half-maximum corresponds to about 16 kev in energy, or 23 percent of the average energy. Not all of this width is due to energy straggling, however; a considerable part is due to angular deviations caused by scattering in the window as is evidenced by the fact that some particles entered the detector at magnet currents greater than the one (marked with an arrow) corresponding to the incident proton energy of 83.5 kev. The relative energy-widths at half-maximum of these profiles are listed in Table II. No correction has been made for the effect of scattering. It will be seen that the relative widths decrease with increasing beam energy, as might be expected.

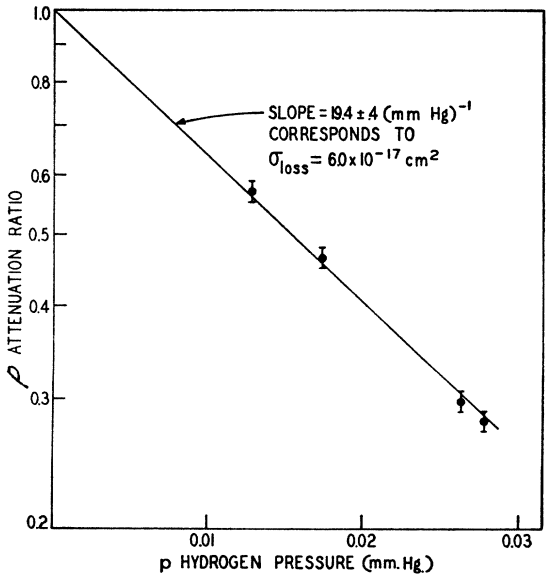

FIG. 4. Attenuation curve at the 0° detector for a 71-kev atomic-hydrogen beam. The magnetic field bends 71-kev protons with a radius of curvature of 5.6 cm.

From these data on the proton kinetic energies before and after the entrance window, energy losses in the window for protons of various incident energies could be estimated. Since no attempt was made to make the windows identical to one another, the losses varied somewhat from window to window. They were always, however, of a reasonable order of magnitude, when compared with those calculated from the data of Warshaw.[19] The actual losses varied from 8 to 15 kv in the various foils used; they are listed in the last column of Table II.

(B) Measurement of Loss Cross Section

To determine the loss cross section it was necessary to measure the attenuation ratio ρ, which is defined in Eq. (1). If we define $r(p)$ as the normalized current to the zero-degree detector (i.e., the ratio of simultaneous readings of detector-galvanometer deflection and monitor-galvanometer deflection) at hydrogen pressure p, then, clearly

$$\rho(p)=r(p)/r(0), \tag{2}$$

where $r(0)$ is the value of r at zero hydrogen pressure. As used in this discussion, the term "zero hydrogen pressure" means a total pressure in the electron-exchange chamber of less than 0.2 micron, so that the hydrogen atom's mean free path for electron loss is greater than ten times the distance between entrance window and the detector.

For the loss cross-section measurement the magnetic field was adjusted to a suitable value, which was never less than that required to bend the protons leaving the window into the 60° detector (a radius of curvature of 11.0 cm). Valve V_1 was opened and the electron-exchange chamber evacuated to a pressure of less than 0.2 micron. At least four measurements of $r(0)$ were taken and averaged. Valve V_1 was then closed and the chamber was filled with hydrogen gas to a desired pressure, generally in the range from five to eighty microns. The gas was assumed to be approximately at room temperature, since a calculation showed that

[19] S. D. Warshaw, Phys. Rev. **76**, 1759 (1949).

temperature equilibrium between the chamber walls and the initially hot gas should be reached in considerably less than one second. At least five measurements of r were made and averaged, and at the same time the gas pressure was read with the McLeod gauge. Finally, V_1 was reopened and $r(0)$ measured again. The value of $\rho(p)$ was calculated by dividing $r(p)$ by the average of the two values of $r(0)$ taken before and after the determination of $r(p)$. This was done in order to take some account of changes (rarely more than five percent) which occurred in successive readings of $r(0)$

At a given beam energy the quantity ρ was determined for at least three hydrogen pressures. A plot was then made of $\log_{10}\rho$ *versus* hydrogen pressure p. From Eq. (1) it can be seen that such a plot should result in a straight line passing through the point ($\rho=1$, $p=0$), and of slope s given by

$$s=\sigma_l d/(1.191\times10^{-19}T) \qquad (3)$$

per mm Hg. Generally, the experimental points fell closely on such a line. In any case the slope of the best line through the points which also passed through ($\rho=1$, $p=0$) was determined; and from it the uncorrected value of the loss cross section, σ_l'', was calculated.

One of these "attenuation" curves, i.e., plots of attenuation ratio *versus* hydrogen pressure, is given in Fig. 4. The curve is for a 71-kev neutral beam; during the measurement the magnetic field was set so that 71-kev protons were deflected with a radius of curvature, a, of 5.6 cm. Table I shows how the points for Fig. 4 were calculated from the measured values of the normalized detector current r. The data are entered in the table in the order in which the experimental measurements were made. Note that $r(0)$ stays fairly constant throughout; this behavior was typical of most of the runs. At the bottom of the table the calculation of the uncorrected cross section σ_l'' is shown, and corrections for the change of detector sensitivity with hydrogen pressure and for finite detector slit width (these corrections will be discussed immediately) are added to σ_l'' to give the corrected loss cross section σ_l.

It should be mentioned that, because the kevatron did not focus well at low voltages, atomic beams of kinetic energies less than 90 kev per particle were generally obtained from the kevatron's molecular-ion beam. The molecular ions decompose in the window and each gives two particles having half the energy of the original molecule. Preliminary measurements showed that, within experimental error, no difference could be observed between the cross section determined for atoms coming from the kevatron's proton beam, and that measured for atoms of the same energy but obtained from molecular ions.

TABLE I. Attenuation ratios at various hydrogen pressures for a 71-kev atomic beam and the calculation of the electron loss cross section from these data.[a]

Hydrogen pressure p 10^{-2} mm Hg	Normalized detector current r	Attenuation ratio $\rho(p)=r(p)/\text{mean } r(0)$
<0.02	1.152	
2.64	0.347	0.347/1.165=0.298
<0.02	1.178	
2.80	0.333	0.333/1.178=0.283
<0.02	1.177	
1.74	0.549	0.549/1.180=0.465
<0.02	1.183	
1.28	0.667	0.667/1.173=0.569
<0.02	1.163	

Calculation of the loss cross section:
s = slope of straight line in Fig. 4 = 19.4±0.4 mm^{-1} Hg,
T = room temperature = 297°K,
a = radius of curvature of 71-kev protons in magnetic field = 5.6 cm,
σ_l'' = uncorrected loss cross section = $(1.191/12.70)\cdot10^{-19}Ts$ = $(5.40\pm0.12)\cdot10^{-17}$ cm^2,
$\sigma_l'=\sigma_l''+0.16\times10^{-17}$ cm^2 = 5.56×10^{-17} cm^2,
σ_l = corrected loss cross section = $\sigma_l'(1+0.0284a^{\frac{1}{2}})$ = $(5.95\pm0.14)\cdot10^{-17}$ cm^2.

[a] The data are presented in the order in which they were determined experimentally. They are the data used in plotting Fig. 4.

(C) Corrections to Be Applied to the Cross Sections

(a) *Correction for the Variation of Detector Sensitivity with Hydrogen Pressure*

If the quantity σ_l'' calculated from the slope of one of the attenuation curves is to be interpreted as the true loss cross section (neglecting the correction for slit width), then the following two conditions must be satisfied:

(i) the detector sensitivity (i.e., the galvanometer deflection per particle entering the detector) must be independent of the strength of the beam, and

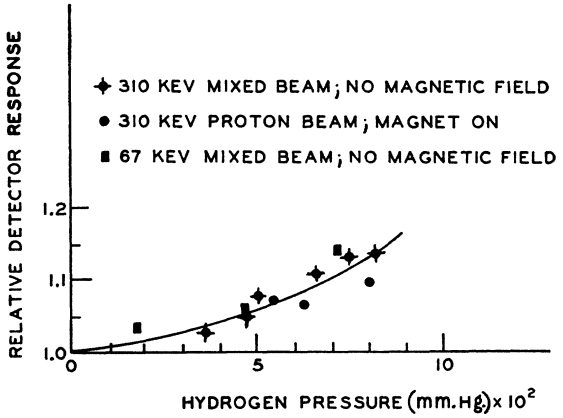

FIG. 5. Variation of detector response with hydrogen pressure.

(ii) the detector sensitivity must be independent of the hydrogen pressure in the detector.

Variations of detector sensitivity with magnetic field, bias voltage on the collecting plate, etc., will not put σ_l'' in error, since these quantities were kept constant during a cross-section measurement.

For the zero-degree detector, operated with its collector at -67.5 v with respect to ground, condition (i) is almost certainly met. Provided that the kevatron beam was sufficiently defocused so that no portions of it had high local intensities, the currents to detector and monitor were found to vary together quite consistently. Condition (ii) was not satisfied, however. Figure 5 shows the variation of detector sensitivity with hydrogen pressure when the 67.5-volt negative bias was used on the collector plate. The ordinate is the relative detector response and is defined as the ratio of the detector sensitivity at hydrogen pressure p to that at hydrogen pressure zero. The points indicated by crosses and by squares were taken with zero magnetic field across the electron-exchange chamber so that both protons and neutral atoms (i.e., a "mixed" beam) entered the detector. Because the magnetic field was zero, loss processes no longer affected the normalized detector current r appreciably, so any observed change in r must be due to a change in detector sensitivity. Thus, the relative detector response at hydrogen pressure p was here measured as the ratio $r(p)/r(0)$. It will be noticed that the relative detector response increases slightly with increasing hydrogen pressure and that at a given hydrogen pressure it is essentially independent of the energy of the incoming protons. This last fact indicates that Rutherford scattering of the beam particles by the hydrogen nuclei in the chamber was negligible—if it were not, one would expect the relative detector response to decrease with decreasing proton energy.

The points indicated by circles on the graph were taken on the 60° detector into which a 305-kev proton beam was being deflected by the magnetic field; the relative detector response again was calculated as the ratio of normalized detector currents. The behavior is seen to be very nearly the same as at the zero-degree detector with a mixed beam entering it and zero field. This shows that the effect is approximately independent of the magnetic field. The slope of the 60° detector curve was found to decrease with decreasing beam energy, however. This change was small for beam energies greater than 200 kev, and it can probably be attributed to capture processes attenuating the beam entering the detector. It is clear that protons which capture an electron during their passage through the hydrogen gas will no longer be deflected by the magnetic field and so will miss the 60° detector slit. Since the capture cross section decreases with a high negative power of the proton energy,[20] the attenuation due to capture processes should do likewise.

From the preceding paragraphs it may be seen that, when a detector is used with its collector plate biased 67.5 v negatively, its response varies slightly with hydrogen pressure; but this behavior is effectively independent of the beam energy and the magnetic field strength. Such a variation is explainable, for the positive slope of the curve in Fig. 5 could be due to ionization of the gas in the detector by incoming protons or atoms or by secondary electrons. The change of detector response with hydrogen pressure was found to correspond to a "cross section" of about -0.16×10^{-17} cm^2. Thus, to take this behavior into account, $(0.16\pm0.05)\times10^{-17}$ cm^2 was added to the uncorrected loss cross section σ_l'', i.e.,

$$\sigma_l'=\sigma_l''+(0.16\pm0.05)\times10^{-17}\text{ cm}^2 \qquad (4)$$

where σ_l' is the cross section corrected for detector response changes.

(b) *Correction for Slit Width*

If the angular aperture defined by the zero-degree detector's entrance slit had been infinitesimally small, all neutral particles which had lost their planetary electron before entering the slit would have been prevented from entering by the magnetic field. For a slit of width w, however, particles changing charge at a distance from the detector of less than b will not be deflected enough by the magnetic field to miss the slit, and will therefore be detected. The distance b clearly depends upon the horizontal displacement of the particle from the detector axis; its average value is given approximately by

$$(b)_{\text{Av}}=(1/w)\int_0^w(2ax)^{\frac{1}{2}}dx=\tfrac{2}{3}(2aw)^{\frac{1}{2}}, \qquad (5)$$

where a is the radius of curvature with which the charged particles are deflected by the magnetic field. This means that the path length between the entrance window and the detector is effectively shortened by a distance b, and so the observed cross section is too small. The true cross section σ_l, is given by

$$\sigma_l=\sigma_l'(1+0.0284a^{\frac{1}{2}}). \qquad (6)$$

In the derivation of this formula it has been assumed that the secondary-electron emission of beryllium-copper is the same for protons and hydrogen atoms at the same energy,[21] and that it is sufficiently large so

[20] N. Bohr, reference 2, pp. 111 ff.

[21] H. W. Berry [Phys. Rev. 74, 848 (1948)] has found that the secondary electron emission of tantalum is about fifty percent higher when it is bombarded by neutral helium atoms than when the incident particles are helium ions of the same energy. The energies in his work were less than four kev. If, in the present case, the secondary electron emission of beryllium-copper is greater for incident hydrogen atoms than for incident hydrogen ions of the same energy, the correction factor given in Eq. (6) would be too large.

that no account need be taken of the current brought to the collector plate by the positive ions resulting from neutral atoms which have changed charge but still enter the detector.

(c) *The Effect of Scattering in the Entrance Window*

Scattering in the entrance window was found to put the observed cross section considerably in error, at least at low proton energies. Neutral particles scattered in the direction away from the 60° detector can be bent into the zero-degree detector by the magnetic field if they change charge at the proper spot. They thus cause the observed cross section to be too low, and a little consideration shows that the effect can be quite large. The purpose of the baffle B (Fig. 1) was to prevent such particles from entering the detector. The mere introduction of the baffle increased the observed cross sections at some energies by as much as 50 percent, even when the same magnetic field was used in both determinations. Note that the baffle was placed sufficiently far (3.2 cm) from the detector so that no neutral changing charge on the knife edge could enter the detector if the magnetic field was not less than that which bends the protons with 11.0-cm radius of curvature.

As the magnetic field is increased, charged particles are removed more effectively from the neutral beam, and the error introduced by scattering becomes smaller. Thus, one would expect the observed cross section to increase with magnetic field. This effect was indeed found at lower beam energies. It was, however, always possible to reach a point at which further increases in the field strength no longer affected the observed cross section, within experimental error. The value of σ_l on such a plateau was then taken as the true loss cross section for the energy in question. At higher beam energies (this includes all but the two lowest energies for which a cross section measurement is given) the measured cross section was found to be essentially independent of the magnetic field, owing to the decrease in scattering with increasing energy. This independence is illustrated in Fig. 6 for atomic beams of two different energies. The abcissas in the figure are the radii of curvature through which a proton beam of energy equal to that of the atomic beam in question (71 kev for curve A and 123 kev for curve B) would be deflected by the applied magnetic field in which the cross-section measurement was made. These radii of curvature are plotted on a reciprocal scale, so that the magnetic field increases linearly toward the right. Note, however, that the magnetic field at a given radius of curvature is not the same for both curves A and B.

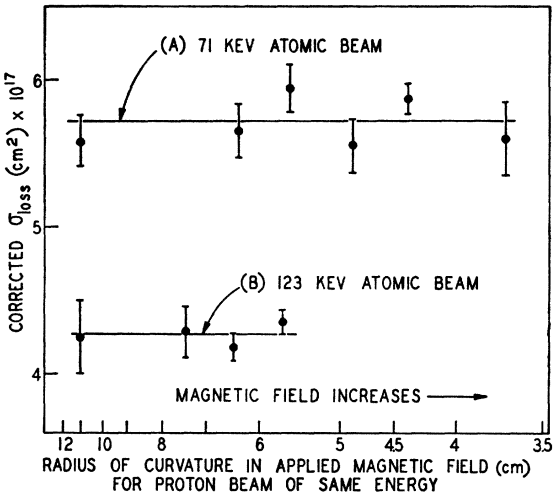

FIG. 6. Plot showing the measured cross section's independence of the magnetic field strength.

(D) Sources of Error

The limits of error indicated in Table II for the measured cross sections were estimated from the scatter of points on the attenuation curves, and on the curves of cross section *versus* magnetic field. They thus take into account errors due to inhomogeneity of the beam and to fluctuation of experimental conditions, reading errors, etc. These errors are essentially random. There are also, however, several sources of systematic error, of which the following are probably the most important.

(i) *Corrections applied to the cross section:* These corrections might be an error because of invalid assumptions made in calculating them. Since the corrections are usually about 10 percent of the measured cross section, the error in the cross section due to such invalid assumptions could hardly amount to more than 5 percent.

(ii) *McLeod gauge calibration:* The McLeod gauge was calibrated by measuring the volumes of its bulb and capillary. The experimental error in the calibration was less than one percent. Since an error in the gauge calibration affects all the measured cross sections by the same percentage, this means that the systematic error in the results due to McLeod gauge calibration errors is less than one percent.

(iii) *Energy straggling in the entrance window:* This effect was considerable at low beam energy, and because of it measurements at energies less than 45 kev were not considered reliable. It decreases fairly rapidly as the energy increases, however, and so should introduce a systematic error which decreases with increasing energy. For a given cross-section measurement this error is probably not greater than the difference between the measured cross section and the cross section (read from the curve in Fig. 7) for an atomic beam equal in energy to the proton beam incident on the entrance window. When this criterion is used, it is estimated that the straggling could not put any of the quoted cross sections in error by more than 5 percent.

IV. RESULTS

The experimental values of the electron loss cross section at various atomic beam energies are given in Table II, and are plotted as a function of beam energy in Fig. 7. The limits of error on the absolute values of the cross section are estimated to be plus or minus 10 percent. (The errors indicated in the table represent

TABLE II. Experimental values of the electron loss cross section per atom for a hydrogen atomic beam passing through hydrogen gas at various atomic beam energies.

Energy per particle in H atomic beam E (kev)	Loss cross section (10^{-17} cm^2)	Relative energy-width at half-maximum of detector current *vs* monitor current profile[a] (percent)	Energy loss in the entrance window (kev)
44.5	6.68±0.23	32	9.2
50.8	6.42±0.20	37	16
70.5	5.72±0.22	23	13.5
112	4.71±0.11	15	8.3
123	4.26±0.09	15	8.5
153	3.80±0.10	14	7.0
204	3.21±0.12	16	9.8
263	2.78±0.10	9	11.0
305	2.38±0.13	11	13.8
321	2.25±0.12	11	23

[a] The values are determined as shown in Fig. 3. They are larger than the width due to energy straggling alone, since they are uncorrected for angular deviations produced by scattering in the entrance window.

random error only and do not include the systematic errors which were discussed previously.) However, the relative values are probably good within 5 percent, as evidenced by the smooth curve on which the points lie in Fig. 7. No results are presented for energies less than 45 kev because of the excessive energy straggling in the foil which occurred at such energies.

Figure 7 is a logarithmic plot of the electron loss cross section *versus* beam energy. Between particle energies of 120 kev and 330 kev, the experimental points may be seen to lie approximately on a straight line, of slope -0.70 ± 0.05. Therefore,

$$\sigma_l \sim E^{-(0.70\pm0.05)}, \quad 120 \text{ kev} < E < 330 \text{ kev}, \tag{7}$$

where E is the hydrogen atom energy.

Bartels[5] gives values of the mean free path for electron capture and of the equilibrium ratio of the charged to neutral component for hydrogen ion beams of energy less than 35 kev passing through hydrogen gas. From the first of these quantities σ_c, the electron capture cross section, can be calculated; the second is equal to σ_l/σ_c. Values of the loss cross section have been computed from these data, and are plotted as circles on Fig. 7.

Meyer,[6] using the same method as Bartels, has given values of σ_l for hydrogen atoms of energies between 35 kev and 150 kev passing through hydrogen gas. The cross sections range from 13×10^{-17} cm^2 at 35 kev to 20×10^{-17} cm^2 at 150 kev with indicated errors of about 15 percent. Such values disagree both with the present data and with those of Bartels. In particular, it hardly seems possible that the dependence of σ_l on energy that has been obtained from the present work could be so radically in error.

In evaluating the present results it should be noted that the method used by Meyer and by Bartels does not allow either cross section to be measured directly; their loss cross-section values are calculated from data directly concerned with the ratio of charged ions to neutral atoms in a beam. The advantage of the present

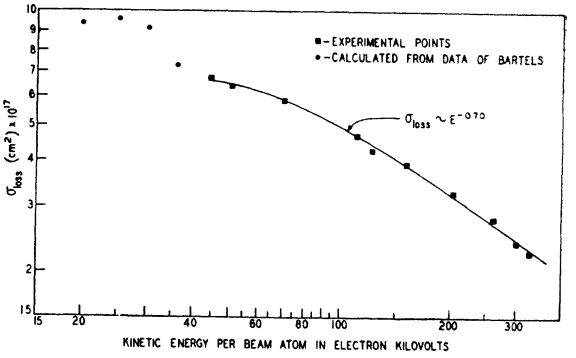

FIG. 7. Logarithmic plot of the electron loss cross section per hydrogen atom for a hydrogen atomic beam passing through hydrogen gas, as a function of beam energy.

method is that it provides a direct measurement of the loss cross section.

Bohr[21] has derived the following expression for σ_l in terms of particle energy:

$$\sigma_l = 4\pi a_0^2 z_1^{-2}(z_2^2+z_2)(E_0/E), \quad E \gg E_0, \; z_1, z_2 \text{ small}, \tag{8}$$

where $a_0=\hbar^2/\mu e^2$ is the Bohr radius, z_1 is the atomic number of the moving particle, and z_2 the atomic number of the substance penetrated. E_0 is that energy at which the particle's velocity is equal to the velocity of an electron in the first Bohr orbit; it equals 24.8 kev for a hydrogen atom. For hydrogen atoms moving through gas, Eq. (8) reduces to

$$\sigma_l = 8\pi a_0^2(E/E_0). \quad E \gg E_0 \tag{9}$$

For $E=245$ kev, Eq. (9) gives $\sigma_l=8.0\times10^{-17}$ cm^2, which is to be compared with 2.8×10^{-17} cm^2 from the present data. In making the comparison it should be remembered that, for 245-kev hydrogen atoms, $E\sim10E_0$. This is hardly a case of $E\gg E_0$, which is the range of validity of Eq. (9). Equation (9) also predicts that $\sigma_l\sim E^{-1}$, which is not far removed from the experimental result of Eq. (7).

Even though Eq. (8) is not valid at low energies, it might well give a fairly accurate prediction of the dependence of σ_l on z_1 and z_2. Thus, for hydrogen atoms passing through helium ($z_2=2$), cross sections 2.5 times as large as the ones here measured might be expected. It seems important to investigate these points in future work.

The author wishes to thank Professor Samuel K. Allison for suggesting this problem, for extending the facilities of his laboratory, and especially for his constant advice and encouragement, without which this work would not have been completed. Grateful acknowledgment is also made of the invaluable assistance of Mr. Fred Ribe, and of the help of Messrs. David Bushnell, Richard Carlson, Harvey Casson, Herbert Kanner, and Allan Morrish.

[21] N. Bohr, reference 2, p. 109, formula (4.2.3).